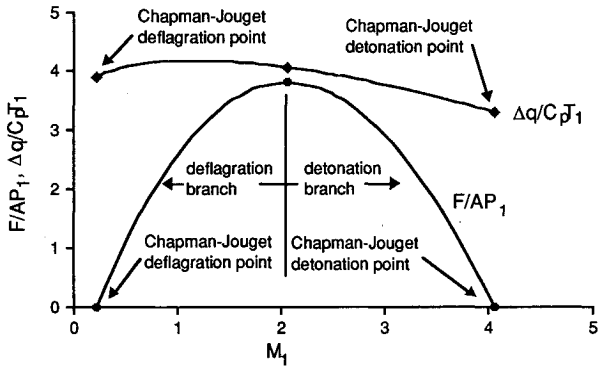

Fig. 2 Sample thrust curve plotted vs. velocity. Reactant mixture is $3CH_4 + 2O_2 + 10N_2$ at initial conditions $P_1 = 51$ atm, $T_1 = 298$ K.

$= \infty$. The presence of the thrust parameter causes the Rayleigh line to pass through the point

$$(v_2/v_1, P_2/P_1) = [1, 1 + (F/AP_1)]$$

shifting it closer to the Hugoniot curve. As the value of the thrust parameter is increased, the two respective solution points in the thermodynamic plane move closer to one another until the maximum thrust value is attained. At this point, the Rayleigh line can be tangent to the Hugoniot curve at only one point

$$(v_2/v_1, P_2/P_1) = [1, 1 + (F/AP_1)|_{max}]$$

and the two solutions collapse to one.

Figure 2 shows the same calculation from Fig. 1, but it is plotted in terms of thrust and energy release as functions of velocity. Not shown in the plot are negative-valued solutions (net drag) that extend from both sides of the curve. The Chapman–Jouget deflagration is never observed in reality and the thrust curve in Fig. 2 provides an explanation for this. A perturbation away from the Chapman–Jouget detonation point will result in a force restoring it to the original velocity while a perturbation away from the Chapman–Jouget deflagration point will result in a force deflecting it further from the original velocity. It is assumed, by analogy, that some portion of the thrust curve near the Chapman–Jouget deflagration point will be physically unrealistic. A method for quantifying this region has not been developed, and so the thrust curve is shown in its entirety.

Conclusions

A quick and efficient method of calculating one-dimensional ram accelerator performance has been developed through modification of the NASA Lewis CET89 computer code. The modified program is best used for analyzing subdetonative ram accelerator propulsion and for evaluating prospective reactant mixtures. Caution has to be exercised when using the results of these calculations because reaction kinetics play a major role in the operation of the ram accelerator where combustion is premixed in nature. One-dimensional theory also fails to predict successful operation above the Chapman–Jouget detonation speed.

References

[1]Bruckner, A. P., Knowlen, C., Hertzberg, A., and Bogdanoff, D. W., "Operational Characteristics of the Thermally Choked Ram Accelerator," *Journal of Propulsion and Power*, Vol. 7, No. 5, 1991, pp. 828–836.

[2]Knowlen, C., and Bruckner, A. P., "A Hugoniot Analysis of the Ram Accelerator," 18th International Symposium on Shock Waves, Sendai, Japan, July 1991.

[3]Chew, G., Knowlen, C., Burnham, E. A., Hertzberg, A., and Bruckner, A. P., "Experiments on Hypersonic Ramjet Propulsion Cycles Using a Ram Accelerator," AIAA Paper 91-2489, June 1991.

[4]Higgins, A. J., Knowlen, C., and Bruckner, A. P., "An Investigation of Ram Accelerator Gas Dynamic Limits," AIAA Paper 93-2181, June 1993.

[5]Nusca, M. J., "Reacting Flow Simulation for a Large Scale Ram Accelerator," AIAA Paper 94-2963, June 1994.

[6]Gordon, S., and McBride, B. J., "Computer Program for Calculation of Complex Chemical Equilibrium Compositions, Rocket Performance, Incident and Reflected Shocks, and Chapman-Jouget Detonations," NASA SP-273, March 1976.

[7]Liberatore, F., "Ram Accelerator Performance Calculations Using a Modified Version of the NASA CET89 Equilibrium Chemistry Code," Army Research Lab. Technical Rept., ARL-TR-647, Dec. 1994.

Performance Comparisons of Low-Power Arcjets

W. D. Deininger,* G. Cruciani,† and M. J. Glogowski‡
BPD Difesa e Spazio, 00034 Colleferro, Rome, Italy

Introduction

ELECTRIC PROPULSION (EP) has recently attracted renewed attention in the space community due to the mass savings and/or payload increases it can provide to geostationary satellites. Although EP has been around for quite a long time, EP systems have been recognized as a mature technology for potential use in space only during the past several years. This is due to several factors. First, extensive EP test programs have not only improved the system performance, but have largely resolved the concerns related to EP integration and compatibility with the spacecraft. A second factor is the competition in the telecommunications satellite community, which pushes satellite subsystems towards higher performance to enhance the satellite capacity. In this sense, EP systems are attractive since they can offer launch mass reductions, increased on-orbit life, and/or payload mass increases that fully justify the development costs. Finally, power generation and storage systems that are now available onboard communications satellites can also provide the power/energy requirements of an EP system.

Two EP system technologies are presently under development in Europe for orbit maintenance of telecommunications satellites: 1) arcjets and 2) ion engines.[1] Low-power arcjets (1 kW-class) can offer substantial propellant mass savings with respect to chemical propulsion systems due to their higher specific impulse. In addition, arcjet systems have a lower dry mass and are less complex than ion engine systems, whereas ion engine systems, based on specific impulse considerations alone, typically provide a larger propellant mass reduction. Arcjet thrusters also minimize spacecraft integration difficulties with monopropellant or bipropellant chemical

Received Aug. 1, 1994; revision received Dec. 16, 1994; accepted for publication Dec. 23, 1994.

*Senior Scientist, Manager Electric Propulsion Laboratory. Corso Garibaldi 22. Senior Member AIAA.

†Physicist, Electric Propulsion Laboratory; currently at Via Bologna 18, 62010 Montecorsaro (MC), Italy.

‡Engineer, Electric Propulsion Laboratory; currently at Pennsylvania State University, Department of Aerospace Engineering, University Park, PA, 16802. Member AIAA.

systems that include hydrazine, whereas ion engine systems require a separate propellant storage and feed system. Therefore, EP systems based on arcjet thrusters are of particular interest and are presently being developed worldwide. Laboratory and advanced development work is ongoing in Italy,[2-4] Germany,[5,6] Japan,[7-9] and the U.S.[10-14] with flight system qualifications completed in the U.S.[14] An arcjet propulsion subsystem is being used operationally for North–South station keeping[15] on the commercial Telstar 4 communications satellite while ion engines will be used for North–South station keeping by Japan and Europe onboard experimental satellites in 1994[16] and 1997,[1] respectively.

This Note describes the design and initial parametric performance test results of an advanced laboratory model arcjet engine designated MOD-B. Data is presented over a specific power range of 16–36 J/mg where specific power is defined as the engine input electrical power divided by the propellant mass flow rate. The specific impulse performance data is also compared to information available in the literature for engines operating at similar conditions.

Facility, Apparatus, and Procedures

The facility used for these tests, designated VP-2, consists of a vacuum plant, power supply system, propellant feed system, data acquisition system, dedicated diagnostics, and laboratory services.[3,4] The vacuum plant is composed of a four-stage, roots blower-based pumping group connected to a 1.6-m-long and 0.8-m-diam steel vacuum chamber. The pumping speed is 19,000 m^3/h at a background pressure of 0.03 mbar during engine operation. Hydrogen and nitrogen are supplied to the facility in the proper ratio to simulate fully decomposed hydrazine. The mass flow rates are measured individually using thermal-type mass flow meters, whereas the total mass flow rate is measured using a coriolis force-type mass flow meter. All flow meters are manufacturer calibrated. Measurements from the coriolis force-type mass flow meter are used in the performance calculations since this meter has exhibited the best reproducibility and accuracy ($\pm 2\%$). The propellant gases are supplied to the engine at an inlet pressure of 1 bar at room temperature. A laboratory power supply system provides a high-voltage pulse of up to 2000 V to start the arcjet, whereas a ballasted power supply provides between 0.5 and 2.0 kW to operate the engine. The engine startup and run voltages are measured using voltage probes, whereas the current is measured using a shunt. The thrust stand is a parallelogram, swing-arm-type device that uses a linear voltage displacement transducer and multiweight calibration system to measure engine thrust with an accuracy of $\pm 5\%$ of the reading. An optical pyrometer with a wavelength range between 0.8–1.1 μm, a temperature measurement range of 600–3000°C, and a spot size of 5 mm is used to measure the temperature along the engine body with an accuracy of ± 10°C.

A schematic of the MOD-B low-power arcjet engine is shown in Fig. 1.[3,4] The engine is designed to better mimic the thermal characteristics of flight-type engines[13,14] than other laboratory model engines being tested elsewhere.[6-8,10-12] The MOD-B engine builds on the experience of a previous engine design, the MOD-A engine,[2,4] and provides flexibility for nozzle, gas injection plate, cathode and heat rejection geometry variations while still maintaining a flight-oriented configuration. The MOD-A nozzle block is made from 2% thoriated-tungsten (2%Th-W) and is expensive to manufacture since it is fairly large. Therefore, a small, low-cost 2%Th-W nozzle insert was designed for the MOD-B engine. The MOD-B nozzle insert is press-fit and lapped into the anode cap. The length and diameter of the molybdenum anode cap can be changed to provide a low-cost method of varying the heat rejection surface area. In addition, the length of the thermal dam is increased compared to the MOD-A engine to further thermally isolate the nozzle region from the rest of the engine and its mounting interface. The engine design forces the propellant to flow through a square helical groove in the outer surface of the internal insulator to regeneratively cool the thermal dam region and preheat the gas. The MOD-B engine is tested with two constrictor geometries: 1) a baseline (B/L) geometry characterized by a diameter of 0.62 mm and a length of 0.64 mm and 2) a second geometry (Geo. 2) with a diameter of 1.02 mm and a length of 0.59 mm. Both engine geometries have conical nozzles with a half-angle of 20 deg and an area ratio of 100.

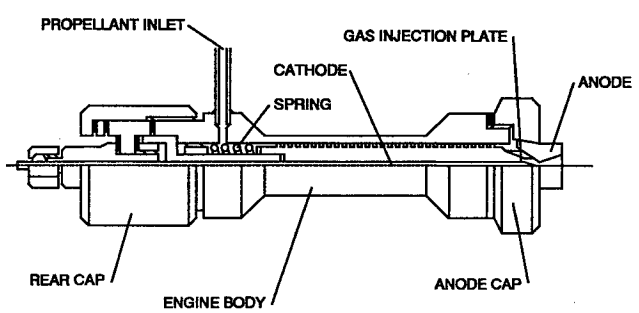

Fig. 1 Schematic of the MOD-B low-power arcjet.

A typical test matrix includes input current values ranging from 8 to 16 A with propellant mass flow rates of 41 and 51 mg/s. The test sequence starts at the highest current and mass flow rate values. After ignition, the engine is allowed to reach steady-state operation and thermal equilibrium (approximately 30 min) before a performance data point is collected. Following data collection, the electrical power and mass flow are turned off simultaneously in order to check the thrust balance zero drift. The engine is then restarted and set up for collection of the next data point.

Results and Discussion

The two MOD-B engine geometries were tested at similar conditions. The voltage drop in the arc was found to be higher for the larger diameter Geo. 2 constrictor, contrary to expectations. For example, at a mass flow rate of 41 mg/s and current values of 15.7 A and 13.8 A, the B/L MOD-B, 0.62-mm-diam configuration had arc voltage drops of 78.5 and 82.7 V, respectively, while at the same conditions, the larger Geo. 2, 1.02-mm-diam constrictor configuration had arc voltage drops of 90.7 and 93.6 V, respectively. The shorter constrictor length coupled to an increased constrictor diameter, which reduces the plenum chamber propellant pressure, should have

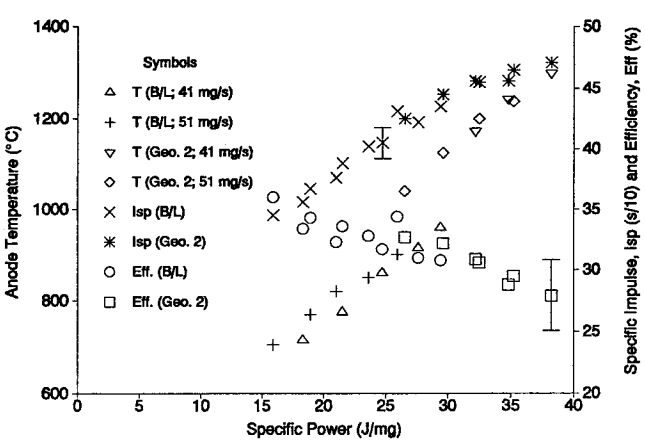

Fig. 2 MOD-B operating characteristics map. (Temperature values have an uncertainty of ±10°C, the Isp, Eff., and specific power have uncertainties of ±5, ±10, and ±2% of the value, respectively. The error bars shown are typical for the Isp and Eff. data points, the symbol size represents the uncertainty in specific power while the symbol size is much greater than the uncertainty for the temperature values.)

resulted in a smaller arc voltage drop. In addition, the Geo. 2 anode with the larger diameter constrictor operated at higher absolute temperatures, as can be seen in Fig. 2, which shows the anode temperature T as a function of specific power. As can be seen, the absolute temperature values at a specific power of 27.5 J/mg differ by approximately 160°C, with the *B/L* MOD-B configuration showing lower temperatures. This temperature difference is believed to be caused by a much smaller surface contact area between the anode insert and radiation cap in the Geo. 2 configuration than in the *B/L* configuration. This is likely caused by the nonrepeatability of the lapping procedure used to seat these two parts. The procedure nonrepeatability will result in a slightly different interference fit that manifests itself as a different surface contact area. A reduced surface contact area results in reduced heat conduction between these parts and causes the anode temperature to increase. Since the anode temperature is known to have a strong dependence on the voltage drop between the electrodes, it is suggested that in this case perhaps the anode temperature variations are affecting the arc voltage drop.

The MOD-B arcjet specific impulse (Isp) and efficiency (Eff.) are also shown in Fig. 2. The specific power ranges from 16 to 36 J/mg for engine input powers of 650–1400 W. The specific impulse varies between 345–471 s over this specific power range, while the engine efficiency ranges from 36 to 29%, respectively. In spite of the different voltage-current and anode thermal characteristics between the two MOD-B geometries, the specific impulse values lay within ±10 s on the specific impulse–specific power characteristic.

A comparison between MOD-B engine operation with data from other researchers is shown in the specific impulse–specific power characteristic of Fig. 3. The data shown from other researchers is from test results with similar vacuum chamber background pressures and propellant inlet conditions (room temperature at 1 bar). References 7 and 10 report data from strictly laboratory model-type arcjets, which feature short engine lengths and thick-walled designs. Short engine lengths preclude the use of regenerative cooling, while the thick walls conduct heat away from the anode, significantly reducing its temperature. These two considerations cause reduced performance due to the lower effective propellant gas temperatures, as can be seen in Fig. 3. Reference 9 reports results from a regeneratively cooled laboratory model arcjet, whereas Ref. 13 reports performance results from an engineering model, flight-type low-power arcjet. As can be seen in Fig. 3, MOD-B arcjet performance is similar to the performance of these two engines, validating the advanced design of the MOD-B engine.

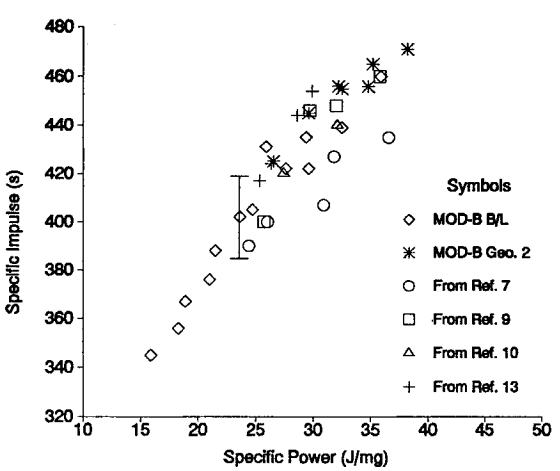

Fig. 3 Comparison of MOD-B performance data with data from the literature. (The Isp and specific power have uncertainties of ±5 and ±2% of the value, respectively, for MOD-B data. The error bars shown are typical for the Isp while the symbol size represents the uncertainty in specific power.)

Summary

An advanced laboratory model low-power arcjet thruster, MOD-B, was tested over an input power range of 650–1400 W. Two MOD-B engine constrictor geometries were investigated and at 24.7 J/mg the baseline configuration gave a specific impulse of 405 s with an efficiency of 31.7% at a mass flow rate of 41 mg/s and an input power of 1.0 kW. The MOD-B arcjet specific impulse–specific power characteristic was compared to data available in the literature for other engines operating at similar test conditions, and was shown to exceed the performance of laboratory engines and to closely mimic the performance of flight-type engines.

Acknowledgments

The activities described in this article were carried out by BPD Difesa e Spazio (BPD) and were sponsored by the European Space Agency (ESA) under European Space Technology and Research Centre (ESTEC) Contract 7632/88/NL/PH through the auspices of the 3rd Advanced Space Technology Programme (ASTP-3). The Contract Technical Monitor for ESA was A. Trippi. The authors would like to thank the reviewers and editors for their constructive criticisms. The MOD-A arcjet was designed by Centrospazio, Consorzio Pisa Ricerche, Pisa, Italy, under Subcontract to BPD.

References

[1]Bartoli, C., "Review of European Activities on Electric Propulsion," *Proceedings of the 22nd International Electric Propulsion Conference*, Vol. 1, Centrospazio, Consorzio Pisa Ricerche, Pisa, Italy, 1991 (IEPC Paper 91-001).

[2]Andrenucci, M., Saccoccia, G., Shultz, U., Scortecci, F., Panattoni, N., and Didier, C., "Performance Study of a Laboratory Model of a Low Power Arcjet," *Proceedings of the 22nd International Electric Propulsion Conference*, Vol. 1, Centrospazio, Consorzio Pisa Ricerche, Pisa, Italy, 1991 (IEPC Paper 91-045).

[3]Cruciani, G., and Deininger, W. D., "Development Testing of a 1 kW Class Arcjet Thruster," AIAA Paper 92-3114, July 1992.

[4]Deininger, W. D., Glogowski, M. J., Cruciani, G., Scortecci, F., and Andrenucci, M., "Comparison of Low Power Arcjet Operation at BPD and Centrospazio," AIAA Paper 92-3115, July 1992.

[5]Glogowski, M., Glocker, B., and Kurtz, H. L., "Experimental Investigation of Radiation and Regeneratively Cooled Low Power Arcjet Thrusters," AIAA Paper 90-2575, July 1990.

[6]Zube, D. M., Glocker, B., Kurtz, H. L., Kinnersley, M., and Matthäus, G., "Development of a Low Power Radiatively Cooled Thermal Arcjet Thruster," *Proceedings of the 22nd International Electric Propulsion Conference*, Vol. 1, Centrospazio, Consorzio Pisa Ricerche, Pisa, Italy, 1991 (IEPC Paper 91-042).

[7]Yoshikawa, T., Onoe, K., Ohba, T., Yoshida, H., Suzuki, H., and Morimoto, S., "Development of a Low Power DC Arcjet for Space Propulsion," AIAA Paper 87-1058, May 1987.

[8]Yoshikawa, T., Onoe, K., Tsuri, S., Ishii, M., and Uematsu, K., "Development of a Low Power Arcjet Thruster—Thrust Performance and Life Evaluation," *Proceedings of the 22nd International Electric Propulsion Conference*, Vol. 1, Centrospazio, Consorzio Pisa Ricerche, Pisa, Italy, 1991 (IEPC Paper 91-043).

[9]Yamada, T., Shimizu, Y., Toki, K., and Kuriki, K., "Thrust Performance of a Regeneratively Cooled Low-Power Arcjet Thruster," *Journal of Propulsion and Power*, Vol. 8, No. 3, 1992, pp. 650–654.

[10]Curran, F. M., and Nakanishi, S., "Low Power DC Arcjet Operation with Hydrogen/Nitrogen Propellant Mixtures," AIAA Paper 86-1505, June 1986.

[11]Curran, F. M., and Haag, T. W., "Extended Life and Performance Test of a Low-Power Arcjet," *Journal of Spacecraft and Rockets*, Vol. 29, No. 4, 1992, pp. 444–452.

[12]Curran, F. M., and Sarmiento, C. J., "Low Power Arcjet Performance Characterization," AIAA Paper 90-2578, July 1990.

[13]Morren, W. E., and Lichon, P. J., "Low-Power Arcjet Test Facility Impacts," AIAA Paper 92-3532, July 1992.

[14]Smith, W. W., Smith, R. D., Yano, S. E., Davies, K., and Lichtin, D., "Low Power Hydrazine Arcjet Flight Qualification," *Proceedings of the 22nd International Electric Propulsion Conference*, Vol. 2, Centrospazio, Consorzio Pisa Ricerche, Pisa, Italy, 1991 (IEPC Paper 91-148).

[15]Marcus, D. J., "AT&T is First to Buy Advanced Thruster on GE Satellites," *Space News*, Jan. 15–21, 1990.

[16]Yoshikawa, T., "Electric Propulsion Research and Development in Japan," *Proceedings of the 22nd International Electric Propulsion Conference*, Vol. 1, Centrospazio, Consorzio Pisa Ricerche, Pisa, Italy, 1991 (IEPC Paper 91-004).

Analysis of Ignition and Flame Spreading in Solid Rocket Motor Star Slots

A. Ciucci,* Rhonald M. Jenkins,† and Winfred A. Foster Jr.‡
Auburn University, Auburn, Alabama 36849

Introduction

THE ignition transient of a solid rocket motor (SRM) employing a pyrogen igniter can be defined as the time interval from the onset of the igniter flow to the time a quasi-steady flow develops. A little-understood portion of the starting transient for (star) slotted head-end grain configurations is the time interval encompassing the initiation of the igniter flow, the first appearance of a flame on the star grain, and the subsequent flame spread over the star slot region.

Previous analyses[1–7] for motors such as those used on the Space Shuttle agree quantitatively well with test data, except for the time period that directly involves burning of the head-end star grain segment. Discrepancies during this time period are believed to arise from three factors: 1) the flowfield is assumed to be one-dimensional, 2) the star geometry in the head-end segment is approximated by variations in port area and grain burning perimeter, and 3) the igniter flowfield is not accounted for.

The authors have previously presented a numerical calculation method utilizing the time-dependent, two-dimensional Navier–Stokes equations, which calculates the subsonic flow induced in the slot by the supersonic igniter plume.[8] The focus of the present study is the calculation of the initial portion of the ignition transient, beginning with the start of igniter flow and ending when the head-end star slot segment of the motor is fully burning. The expanding igniter plume, the complex flow patterns within the star slot, heat transfer to the propellant grain, and subsequent propellant burning are considered.

Analysis

The geometry considered is that of the Space Shuttle SRM, consisting of a head-end, star slot segment and three long circular port (CP) grains. Flow in the head-end slot region is assumed to be two dimensional, whereas that in the downstream CP region is assumed to be axisymmetric. As shown in Fig. 1, several planes of symmetry exist in the head end, corresponding to the number of slots. Reference 8 presents

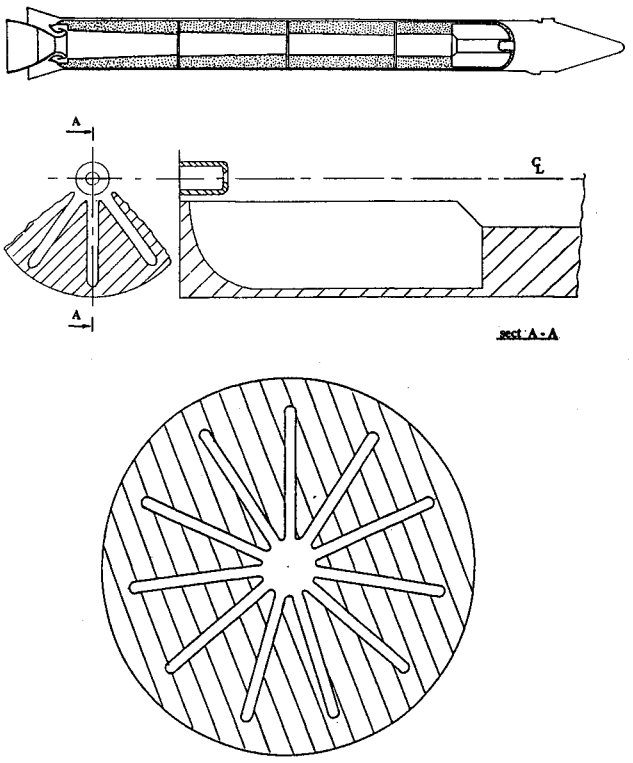

Fig. 1 Geometry of the Space Shuttle SRM star slot.

the full set of governing equations, including appropriate source terms due to propellant burning in both the slot and CP regions. The igniter exit parameters at the condition of maximum igniter mass flow are taken as reference values. The distance from the motor centerline to the bottom of the slot is taken as the reference length.

The purpose of the present analysis is to present a methodology for examination of the interaction between the igniter plume, the developing flowfield within the head-end star grain slots, and the rate of flame spread over the grain surface. Both convective and radiative heat transfer to the propellant grain surface are considered. The convection model utilizes a correlation developed by Kays and Leung,[9] used previously to correlate heat transfer within the O-ring gap of the Space Shuttle nozzle-to-case joint,[10] given by

$$Nu = \frac{0.152Re^{0.9}Pr}{0.833[2.25\sqrt{(0.114Re^{0.9})} + 13.2Pr - 5.8]} \quad (1)$$

where the Reynolds number is based on the hydraulic diameter of a single star grain slot. Comparison of the predictions of this correlation with cold-flow experimental data taken in a one-tenth scale model of the Space Shuttle head-end slot is given in Ref. 10. Following Johnston,[7] we consider only segments of the propellant grain that lie adjacent to burning propellant, assume that the propellant surface absorbs and the flame emits perfectly, and utilize a shape factor of 0.5 for the unignited adjacent segment. This results in the following expression for the radiative heat transfer coefficient:

$$h_r = (\sigma/2)(T_{\text{flame}}^2 + T_{\text{wall}}^2)(T_{\text{flame}} + T_{\text{wall}}) \quad (2)$$

where σ is the Stefan–Boltzmann constant and T_{flame} is the flame temperature. The propellant burning rate is taken as

$$r = r_{\text{ref}}(p/p_{\text{ref}})^n \exp[\sigma_p(T_{p_i} - T_{\text{ref}})] \quad (3)$$

The grain is considered to be a semi-infinite slab whose temperature is initially uniform. Heat transfer to the slab from

Received May 13, 1993; revision received Jan. 30, 1995; accepted for publication Jan. 31, 1995.

*Graduate Research Assistant, Aerospace Engineering Department. Student Member AIAA.

†Associate Professor, Aerospace Engineering Department. Senior Member AIAA.

‡Associate Professor, Aerospace Engineering Department. Associate Fellow AIAA.